Electrochimica Acta 54 (2009) 3671–3676

Contents lists available at ScienceDirect

Electrochimica Acta

journal homepage: www.elsevier.com/locate/electacta

High resolution TEM and triple-axis XRD investigation into porous silicon formed on highly conducting substrates

T.L. Sudesh L. Wijesinghe[a], Shi Qiang Li[a], Mark B.H. Breese[b], Daniel J. Blackwood[a,*]

[a] Department of Materials Science and Engineering, National University of Singapore, Block E3A, 7 Engineering Drive 1, Singapore 117574, Singapore
[b] Department of Physics, National University of Singapore, Block E3A, 7 Engineering Drive 1, Singapore 117542, Singapore

ARTICLE INFO

Article history:
Received 17 October 2008
Received in revised form 5 January 2009
Accepted 17 January 2009
Available online 24 January 2009

Keywords:
Porous silicon
Etching
Lattice parameters
Transmission electron microscopy
Triple-axis X-ray diffraction

ABSTRACT

The microstructure of thin porous silicon films (∼1 μm) formed potentiostatically on p^+-type silicon in dilute HF solutions is investigated via high resolution TEM and triple-axis XRD. Average pore diameters were found to increase with increasing etching potential, changing from a mixture of micro- and mesopores to predominately square macropores once oxide growth commences. It is postulated that these square pores result from crystallographic etching. High resolution TEM images revealed that stresses within porous silicon are sufficient to cause lattice distortions of the order of a few percent and that once oxide formation occurs areal defects are generated. Although the high resolution TEM analysis suggests that the lattices of the majority of the nanocrystals are compressed relative to bulk silicon and explanations for this are proposed, the combination of the porous silicon film's high porosity and thinness meant that this could not be confirmed by the more reliable triple-axis XRD measurements. Conversely, the triple-axis XRD revealed that thicker films grown under the same conditions had expanded lattices. The results also highlight the drawbacks of relying solely on high resolution TEM or double-axis XRD data when investigating the nature of lattice distortions.

© 2009 Elsevier Ltd. All rights reserved.

1. Introduction

The first high resolution transmission electron microscopy (HRTEM) investigation of luminescent porous silicon (PSi) was conducted by Cullis and Canham [1] which, together with subsequent investigations, confirmed the presence of nanocrystals that are less than 5 nm in diameter [2–15]. Martin-Palma et al. [13] used Fourier transform techniques to enhance their HRTEM images to study the interplanar distance in PSi. These authors initially reported lattice expansions of up to 8% for PSi formed on p-type silicon of resistivity 0.1–0.5 Ω cm etched in concentrated HF. However, a more detailed later analysis revealed anisotropy in the nanocrystals; the <1 −1 1> direction showing only lattice expansions, whilst a mixture of expansions and contractions of up to 6% appeared in the <1 −1 −1> direction. This along with observed intersection angles of up to 73.3° promoted these authors to conclude that the structure of PSi is partially triclinic [16]. Further HRTEM investigations lead the same authors to conclude that the high stress found in the PS/Si interface has its origin in a high density of dislocation pairs [7,17].

Likewise the early high resolution X-ray diffraction (XRD) studies by Barla et al. [18] and Young et al. [19] revealed that the PSi lattice layer is expanded in the direction perpendicular to the sample surface causing a tetragonal distortion. Later works showed that the strain increases with both decreasing pore size and substrate conductivity, as well as upon oxidation [20,21]. Similarly XRD measurements on p^+ silicon indicated that the lattice parameter initially increases with etching time, but becomes constant at longer etching times [22,23].

On first thoughts one might not predict a lattice expansion for PSi; after all surface stress causes small particles of most materials to contract. Indeed, calculations suggest that for clean silicon surfaces the average intrinsic surface stress tensor is probably positive (tensile), so small silicon particles should have a lattice parameter contraction [24]. However, electrochemically prepared PSi does not have a clean surface and the often observed lattice parameter expansion has been attributed to the influence of chemisorbed hydrogen [25,26]. Lehmann et al. [4] attributed changes in the lattice parameter to van der Waals forces between adsorb hydrogen inducing a reconstruction of the surface. Likewise oxidation of the PSi, for example in an aged specimen, may also induce stresses that can lead to lattice parameter expansions [19,24].

The aim of this paper is to present the findings of HRTEM and triple-axis XRD investigations into the pore structure and nanocrystal properties, including size and lattice spacings, of luminescent PSi formed on highly conductive p^+-type silicon in dilute HF solutions. It will also be seen that the findings in this paper highlight

* Corresponding author. Tel.: +65 68746289; fax: +65 67763604.
E-mail address: msedjb@nus.edu.sg (D.J. Blackwood).

0013-4686/$ – see front matter © 2009 Elsevier Ltd. All rights reserved.
doi:10.1016/j.electacta.2009.01.045

the drawbacks of relying solely on HRTEM or double-axis XRD data when investigating the nature of lattice distortions.

2. Experimental

PSi was formed on degenerately doped (boron) p+-type, 0.015 Ω cm resistivity (Virginia Semiconductors) (1 0 0) oriented wafers by etching in a solution of 2.7 wt% HF dissolved in a 1:2 mixture of H_2O and ethanol. A standard three electrode system was used with a Si working electrode, a platinum mesh counter electrode and a saturated calomel reference electrode (SCE). The reference electrode was furnished with a polyethylene luggin capillary with the tip positioned at around 5 mm distance from the working electrode. All potentials quoted in this paper are versus SCE and have been corrected for the uncompensated solution resistance (IR drop). The potentiostat and sweep generator components of an ACM Instruments field machine were used to potentiodynamically polarize the silicon wafers at a rate of 5 mV s^{-1} from −1000 mV to the chosen etching potential, which was maintained for 10 min; during the holding period the current density fell by less than 2%. After etching in the HF solution the samples were rinsed in ethanol and blown dry by nitrogen gas and then, to reduce the danger of air oxidation, immediately transferred to a portable vacuum chamber for transportation to the transmission electron microscope or diffractometer. All the PSi films formed showed strong photoluminescence under a 325 nm HeCd laser, as has been previously discussed elsewhere [27].

The HRTEM samples were prepared in a similar manner to that reported by Cullis and Canham [1] except the porous silicon was not allowed to fall directly onto the copper grids. Instead these grids were dipped into ethanol and then touched gently onto the removed PSi, thereby picking it up. The HRTEM used was a JEOL JEM 3010 HRTEM operated at 300 kV. The HRTEM images were analyzed to obtain interplanar (d) spacings, revealed by lattice fringes, using Digital MicroAnalysis software; this applies a fast Fourier transform to the image to form a diffraction pattern, which is then filtered using a mask and then an inverse fast Fourier transform is applied to obtain a clean image. This is the same technique as used previously by Martin-Palma et al. [7,8].

XRD analysis was preformed on a Bruker D8 Discover Diffractometer operated in the triple-axis mode. This mode has the advantage of being able to distinguish between strain induced lattice mismatch (revealed by θ–2θ scans) and layer tilt or misorientation (revealed by rocking curves), something that the double-axis XRD technique used in the majority of previous investigations is unable to do [28].

3. Results and discussion

The current voltage (I–V) curve for 0.015 Ω cm, p+-type silicon anodized in 2.7 wt% HF is shown in Fig. 1, the characteristics of which we have previously discussed in detail [27]. The important features of the curve are the switch from an exponential dependence of the current density on the applied potential to an almost linear relationship, occurring at about 35–40 mV, and a significant decrease in the I–V slope at 90 mV, marking the so called U_{ps} potential that is often considered to be the transition between PSi formation and electropolishing [29–32]. Therefore, TEM investigations were conducted on PSi specimens formed at potentials on either side of these two points, i.e. at 0 mV, 80 mV and 150 mV; the approximate current densities flowing at these formation potentials were 1.4 mA cm^{-2}, 9.5 mA cm^{-2} and 10.5 mA cm^{-2} respectively.

Fig. 2(a)–(c) shows the HRTEM bright field images of PSi structures formed at 0 mV, 80 mV and 150 mV respectively. From these it can be seen that the pore morphology (shape, size and distribution) is affected by the polarizing potential. At 0 mV the maximum pore diameter appears to be 30 nm and around 70% of the pores present per unit area are scaled in the range of 10–20 nm, with only a few pores less than 10 nm. Whereas at 80 mV the maximum pore diameter is close to 50 nm with around 80% between 20 nm and 50 nm. At both these potentials the pores have irregular shapes. However, at 150 mV the pores took on a more regular square shape that measured between 20 nm and 65 nm across the diagonal, with about 70% of these squares being larger than 50 nm. Thus the average pore diameter increased with increasing applied potential, with a mixture of micropore (diameter <2 nm) and mesopore (2 nm < diameter < 50 nm) pores being observed at 0 mV and 80 mV, but mostly macropores (diameter >50 nm) at 150 mV. The present data are thus in agreement with the general trend of increasing porosity with increasing anodizing current density that has been widely reported [2,10,33].

The square pores observed on etching at 150 mV are somewhat similar to, although more regular than, those previously reported for a supercritically dried 95% porosity layer formed on p+ silicon (0.01 Ω cm) in 10% ethanoic HF [33]. However, the present pores are also reminiscent of scanning electron microscope (SEM) images of the (1 0 0) silicon surfaces crystallographically etched either by anodizing in HF/H_2O_2 solutions or chemically by concentrated NaOH. Since 150 mV is above the U_{ps} potential at least a partial oxide should have developed during anodization, perhaps this caused a reduction in the etching rate of the (1 1 1) faces leading to anisotropic etching [29]. Support for possible crystallographic etching was found when the HRTEM was focused on the pore walls, as this revealed the existence of nanocrystals both on their tops and sides suggesting a slanted wall (Fig. 3). Unfortunately, we were not able to obtain an estimation of the pore walls' angle of slope and thus unable to confirm that these were indeed the (1 1 1) faces.

In a previous publication we reported the influence of the formation potential on the dimensions of the resultant nanocrystals [27]. At all potentials a large size range of nanocrystals were seen, from 1.5 nm to 25 nm in diameter. However, as the formation potential became more positive the fraction of the PSi particles that were smaller than 5 nm increased. For the present work the nanocrystals were further investigated by Fourier transforming their HRTEM images to attain reciprocal lattice images, which allowed interplanar distances (d spacings) and intersecting angles within the individual nanocrystals to be obtained. Kohno et al. [14] have pointed out the importance of measuring the intersecting angle besides the d spacings to avoid any misjudgment of the relative

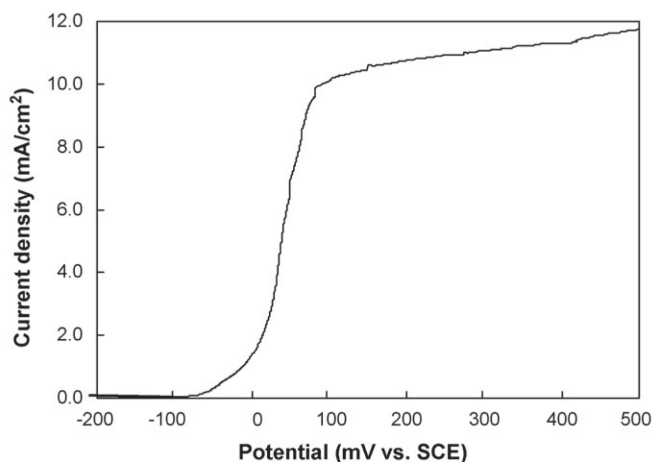

Fig. 1. Potentiodynamic polarisation curve for 0.015 Ω cm p-type etched in 2.7 wt% HF. Curve has been corrected for IR drop.

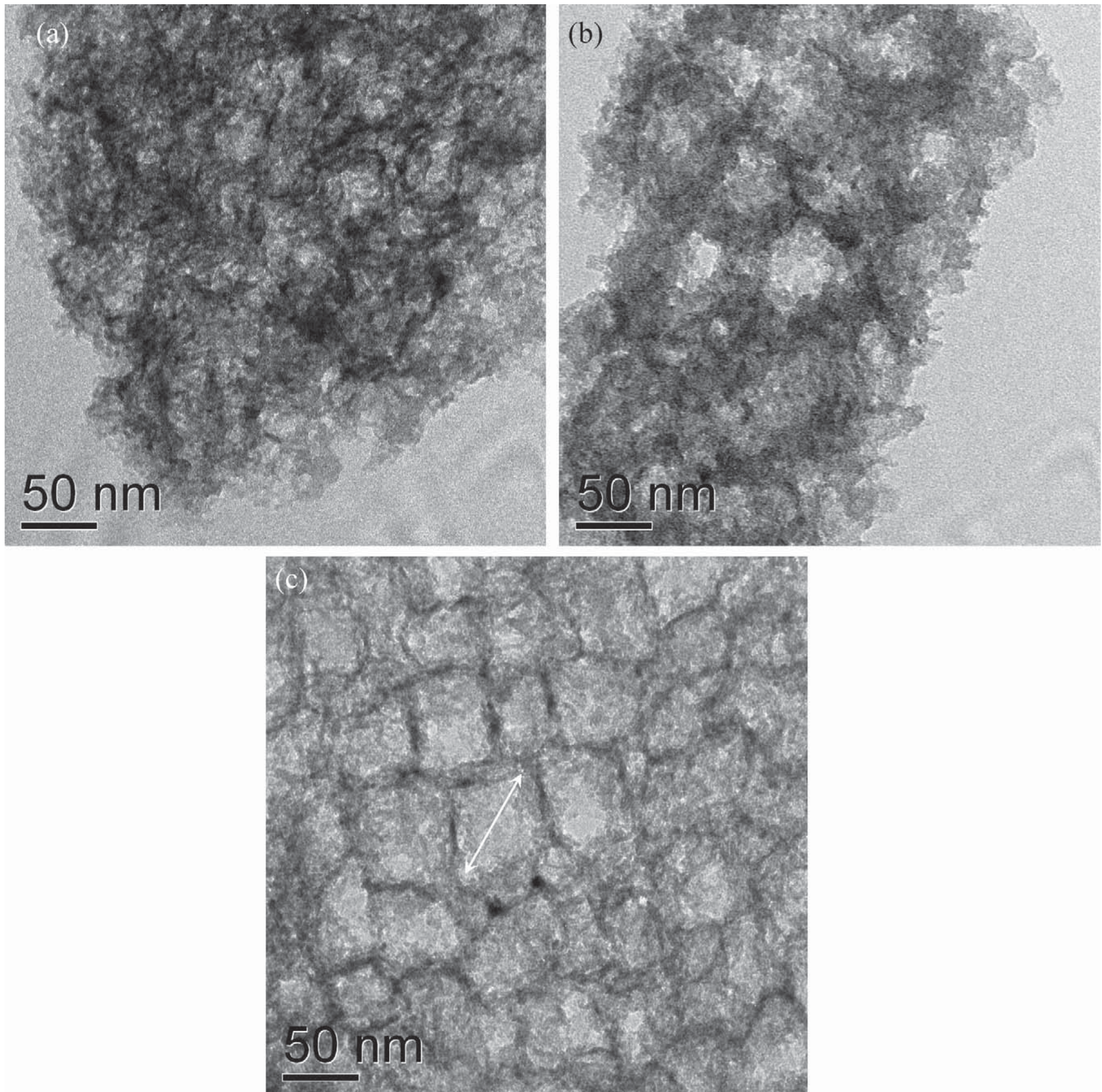

Fig. 2. HRTEM images (bright field) of the pore structure of 0.01 Ω cm p^+-type etched in 2.7 wt% HF at (a) 0 mV; (b) 80 mV and (c) 150 mV. At 150 mV the diagonal dimension of the etch squares was measured, as indicated by the arrow.

plane. The intersecting angles were all within about 1° of 70°, consistent with the {1 1 1} plane.

The interplanar distances measured were found to vary in the range of 2.88–3.12 Å, but no dependence of the *d* spacings on either particle size or etching potential was apparent (note that it was not possible to obtain *d* spacing from nanocrystals with diameters smaller than 2 nm). For the etching potentials the average *d* spacings, along with standard deviations in brackets (σ), were: 0 mV = 2.986 (0.046) Å; 80 mV = 2.981 (0.043) Å; and 150 mV = 2.970 (0.043) Å. When these data are compared to the earlier work by Martin-Palma et al. [7,16] it is found that although the extent of the spread in the *d* spacings at approximately 8% is consistent, the actual magnitudes contrast sharply. In the present work all the *d* spacings are smaller than the expected value for the <1 1 1> direction of bulk silicon at 3.135 Å, i.e. they could be interpreted as indicating a contraction rather than the normally observed expansion. However, unless some internal calibration standard is available, which is not the case with our sample preparation method, the reliability of the accuracy of *d* spacing measurements obtained from HRTEM is poor, so alone they are insufficient to claim a lattice contraction. Nevertheless, the precision with which HRTEM can determine *d* spacings is reliable, so the fact that in the present work these varied by up to 8% from nanocrystal to nanocrystal, even within the same image, means that it is still possible to conclude that the stress within the PSi formed in highly conductive p^+-type silicon is sufficient to cause lattice distortions of the order of a few percent.

Further evidence of this lattice distortion can be seen in Fig. 4 that shows an areal defect, most likely a stacking fault, inside a nanocrystal formed at 150 mV. Of the three formation potentials,

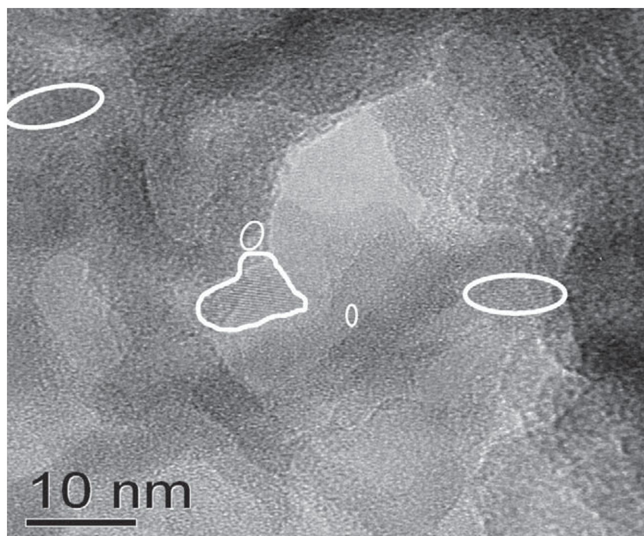

Fig. 3. HRTEM image focused on the pore walls of a PSi sample formed at 150 mV. Note the existence of nanocrystals both on their tops and sides suggesting a slanted wall.

such defects were only observed in the PSi formed at 150 mV and not in those specimens grown at the two lower potentials. Since 150 mV is above the U_{ps} potential the areal defects may have been induced by oxide formation, which can cause high strains in the PSi [24,34].

Previously, contractions of the lattice parameter of PSi have only been reported: (i) after high temperature annealing (>350°C), explained in terms of desorption of the surface hydrogen or recrystalization of amorphous regions [25,35,36]; or (ii) in the presence of low pressure hydrocarbons, explained in terms of attractive van der Waals interactions within the nanometer-size cavities, which increase when the walls are covered by a thin liquid film; for this reason pentane drying was avoided in the present set of experiments [37,38]. Hence lattice contractions had not been expected in the present PSi samples.

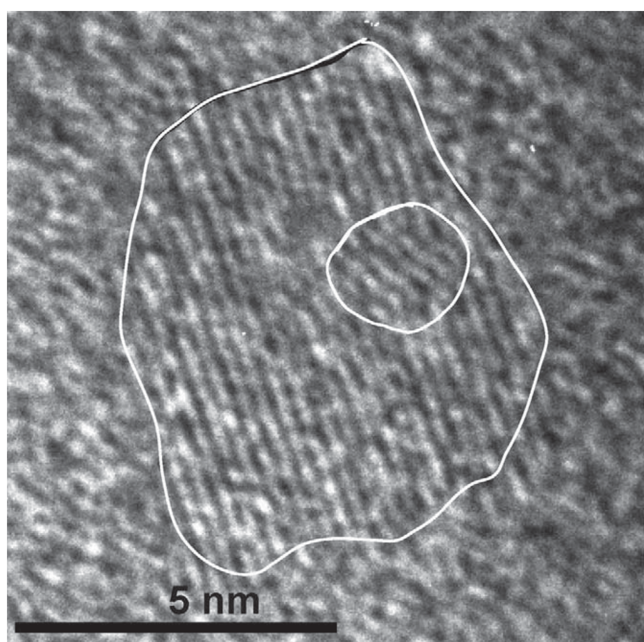

Fig. 4. Areal defect in a silicon nanocrystal (circled) found in PSi formed at 150 mV.

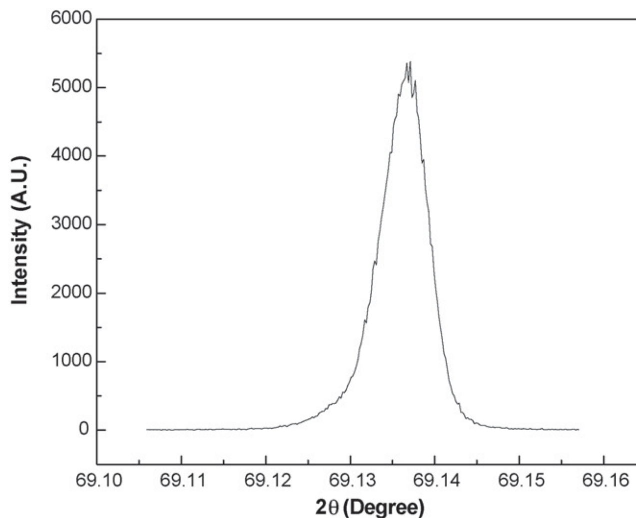

Fig. 5. Triple-axis θ–2θ XRD pattern around the (0 0 4) reflection for a PSi sample formed at 80 mV.

Therefore to ascertain whether the lattice distortions revealed by the HRTEM were really contractions, triple-axis XRD was preformed in the θ–2θ mode about the (0 0 4) reflection. Fig. 5 is a triple-axis θ–2θ pattern for a PSi sample formed at 80 mV, it shows only a single peak at the position for bulk Si substrate, this implies that the average lattice parameter of the PSi in the sample is the same as that of bulk silicon i.e. neither a contraction nor an expansion. It is interesting to note that a triple-axis rocking curve from the same sample used for the θ–2θ pattern does show an additional peak at a separation of about 0.01°, which is caused by tilting of crystal planes in the bulk substrate (Fig. 6). Similar XRD rocking curve patterns could be obtained from fresh silicon wafers, i.e. without any PSi layer, confirming that the second peak is not related to the PSi. The magnitude of the peak separations from these fresh samples varied from wafer to wafer, but in some cases it was as high as 0.05°. This is of the same magnitude as that reported for lattice distortions in double-axis scans, which suggests that some of these earlier observations may have in fact been due to tilting.

It is possible that because the PSi films grown in this work were both highly porous and very thin (approximately 1 μm according

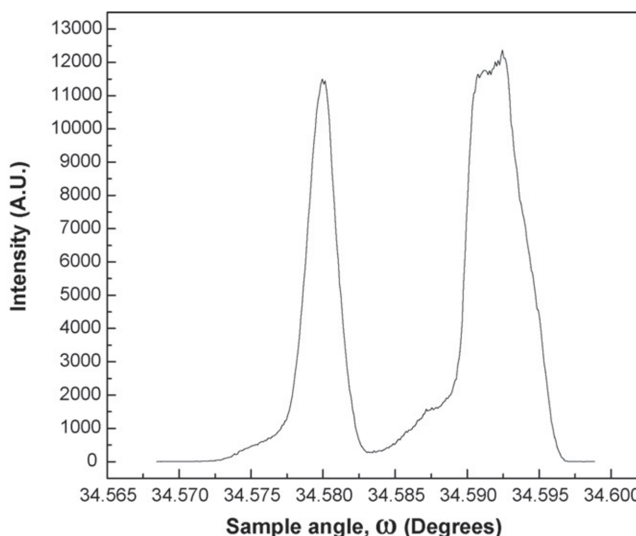

Fig. 6. Triple-axis XRD rocking curve about the (0 0 4) reflection for a sample formed at 80 mV. The second peak is due to tilting of crystal planes, similar patterns are obtained on fresh Si wafers without any PSi layer.

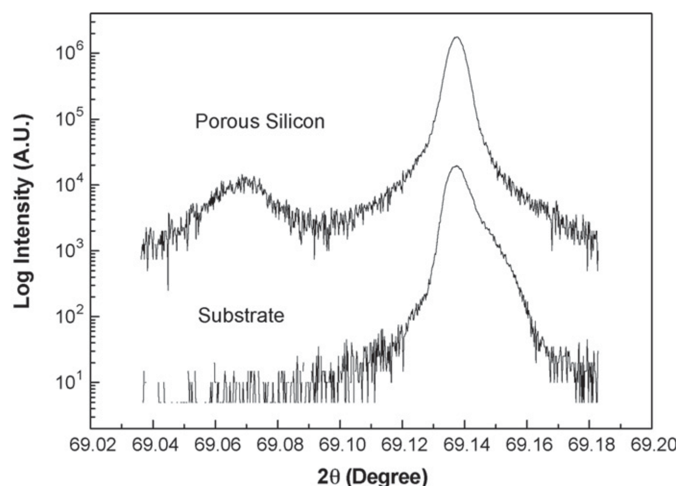

Fig. 7. Triple-axis θ–2θ XRD pattern around the (0 0 4) reflection for a PSi sample formed at 80 mV for the longer time of 2 h (as opposed to 10 min) along with the equivalent pattern for a bare Si wafer.

to cross-sectional SEM images) they could not be detected in the triple-axis XRD pattern shown in Fig. 5. Therefore, thicker films were formed by maintaining the etching potential for 2 h, instead of the original 10 min. Fig. 7 shows for these films triple-axis θ–2θ XRD now yields the anticipated two peaks for the (0 0 4) reflection, however, the weaker band that belongs to the PSi layer has the smaller diffraction angle corresponding to a lattice expansion. Nevertheless, the change in the 2θ angle of 0.068° represents a lattice expansion ($\Delta a/a$) of 4.6×10^{-4}, which is consistent with the magnitudes of previous reports [18–22].

Nevertheless, there remains the possibility that the extent of the lattice expansion increases with film thickness, i.e. although the thick film (~12 μm) grown for the triple-axis XRD certainly had lattice expansion, this does not completely rule out the possibility that the original thin film (~1 μm) used in the HRTEM study had a lattice contraction. Pascual et al. [16] have previously reported that the extent of lattice expansion in PSi films varies with depth. Furthermore, when one considers the causes of the lattice expansion (as described in the introduction section) there are reasons why the PSi grown in the present work could have a much smaller lattice expansion, or even a contraction, than those reported in previous studies. To start with, in the current work care was taken to minimize the PSi's exposure to atmospheric oxygen, since oxidation is known to result in stresses that lead to lattice expansion [15]. Wolkin et al. [39] found that PSi can oxidize within a few minutes, so it is likely that at least some of the previous studies were conducted on at least partially oxidized samples. For example, Martin-Palma et al. [17] found relatively high levels of oxygen in the PSi used in their HRTEM experiments, which might indicate that the large lattice expansions they observed were in part due to oxidation.

In addition, the experimental conditions used in the present work are different from previous works in two important aspects. Firstly, at 0.015 Ω cm the present silicon wafers were at least an order of magnitude more conductive and it has been reported that the extent of the lattice expansion decreases with increasing conductivity [18,19]. Secondly, at 2.7 wt% the HF concentration was much lower than the typical >20 wt% used in most other works. A consequence of the low HF concentration was that the formation current density never exceeded 10.5 mA cm^{-2}, as higher values result in electropolishing. In turn this means that the electric fields applied during PSi formation in the present experiments were lower than in many other works. This is significant as Martin-Palma et al. [7] previously proposed that these fields play an important role in distorting the Si unit cell. Note that a low HF concentration was chosen for the present work as it was desired to grow PSi under potentiostatic control and it is difficult (dangerous) to use a reference electrode system in concentrated HF.

From the preceding two paragraphs, it appears that the forces that lead to lattice parameter expansion are likely to be much smaller in the present case than in most of the previous works. This may have allowed these forces to be balanced, or even out-weighed, by the surface stresses that normally cause small particles to contract giving rise to a mixture of PSi nanocrystals with expanded and contracted lattices.

Finally, it is known that doping will shift a semiconductor's lattice parameter away from its intrinsic value, with boron in silicon causing a contraction. However, the work of Kucytowski and Wokulska showed that at the doping levels required for a resistivity of 0.015 Ω cm (approx. 5×10^{18} cm^{-3}) the lattice parameter contraction is only of the order of 3×10^{-5} [40]. This is an order of magnitude smaller than the lattice distortions observed in PSi, so this phenomenon cannot explain the apparent contractions observed under the HRTEM.

4. Conclusion

The microstructure of thin PSi films (~1 μm) formed potentiostatically on highly conductive p$^+$-type silicon (0.015 Ω cm) in dilute HF solutions was investigated via HRTEM and triple-axis XRD. The average pore diameter increased with increasing applied potential, with a change from a mixture of micro- and mesopores to predominately square macropores, with slanted walls occurring as the U_{ps} potential was exceeded. It is postulated that these square pores are evidence of crystallographic etching.

The HRTEM revealed that stresses within PSi are sufficient to cause lattice distortions of the order of a few percent and once oxide formation occurs (above U_{ps}) areal defects are generated. Although the HRTEM analysis also suggested that the lattices of the majority of the nanocrystals were compressed relative to bulk silicon, a combination of the PSi films' high porosity and thinness meant that that this could not be confirmed by the more reliable triple-axis XRD measurements. Conversely, triple-axis XRD revealed that thicker PSi films grown under the same conditions had expanded lattices, suggesting that the apparent lattices contractions seen in the HRTEM could be due to the lack of an internal calibration standard. These results also highlight the drawbacks of relying solely on HRTEM or double-axis XRD data when investigating the nature of lattice distortions.

Acknowledgement

Financial support was provided by the Agency for Science, Technology and Research (A*STAR) under grant number 0421010083.

Appendix A. Supplementary data

Supplementary data associated with this article can be found, in the online version, at doi:10.1016/j.electacta.2009.01.045.

References

[1] A.G. Cullis, L.T. Canham, Nature 353 (1991) 335.
[2] N. Noguchi, I. Suemune, M. Yamanishi, G.C. Hua, N. Otsuka, Jpn. J. Appl. Phys. 31 (1992) L490.
[3] K.H. Jung, S. Shih, D.L. Kwong, T. George, T.L. Lin, H.Y. Liu, J. Zavada, J. Electrochem. Soc. 139 (1992) 3363.
[4] V. Lehmann, B. Jobst, T. Muschik, A. Kux, V. Petrova-Koch, Jpn. J. Appl. Phys. 32 (1993) 2095.
[5] A. Nakajima, Y. Ohshima, T. Itakura, Y. Goto, Appl. Phys. Lett. 62 (1993) 2631.
[6] O. Teschke, M.C. Goncalves, F. Galembeck, Appl. Phys. Lett. 63 (1993) 1348.
[7] R.J. Martin-Palma, L. Pascual, A.R. Landa-Cánovas, P. Herrero, J.M. Martines-Duart, Mater. Sci. Eng. C 25 (2005) 595.

[8] R.J. Martin-Palma, L. Pascual, P. Herrero, J.M. Martines-Duart, Appl. Phys. Lett. 81 (2002) 25.
[9] M. Song, Y. Fukuda, K. Furuya, Micron 31 (2000) 429.
[10] D.J. Lockwood, A.G. Wang, Solid State Commun. 94 (1995) 905.
[11] L. Pavesi, G. Giebel, F. Ziglio, G. Mariotto, F. Priola, S.U. Campisano, S. Spinella, Appl. Phys. Lett. 65 (1994) 2182.
[12] S.-F. Chuang, S.D. Collins, R.L. Smith, Appl. Phys. Lett. 55 (1989) 675.
[13] A. Parisini, R. Angelucci, L. Dori, A. Poggi, P. Maccagnani, G.C. Cardinali, G. Amato, G. Lerondel, D. Midellino, Micron 31 (2000) 223.
[14] H. Kohno, N. Ozaki, H. Yoshida, K. Tanaka, S. Takeda, Cryst. Res. Technol. 38 (2003) 1082.
[15] A.G. Cullis, L.T. Canham, P.D.J. Calcott, J. Appl. Phys. 82 (1997) 909.
[16] L. Pascual, R.J. Martin-Palma, A.R. Landa-Canovas, P. Herrero, J.M. Martinez-Duart, Appl. Phys. Lett. 87 (2005) 251921.
[17] R.J. Martin-Palma, L. Pascual, A.R. Landa-Canovas, P. Herrero, J.M. Martinez-Duart, Mater. Sci. Eng. C 26 (2006) 830.
[18] K. Barla, R. Herino, G. Bomchil, J.C. Pfister, A. Freund, J. Cryst. Growth 68 (1984) 727.
[19] I.M. Young, M.I.J. Beale, J.D. Benjamin, Appl. Phys. Lett. 46 (1985) 1133.
[20] T. Maehama, C. Afuso, N. Itoh, Jpn. J. Appl. Phys. 37 (1998) 998.
[21] D. Bellet, G. Dolino, Thin Solid Films 276 (1998) 1.
[22] V. Chamard, C. Pichat, G. Dolino, Euro. Phys. J. B 21 (2001) 185.
[23] D. Bellet, S. Billat, G. Dolino, M. Ligeon, C. Meyer, F. Muller, Solid State Commun. 86 (1993) 51.
[24] D. Buttard, D. Bellet, G. Dolino, J. Appl. Phys. 79 (1996) 8060.
[25] H. Sugiyama, O. Nittono, J. Crystal Growth 103 (1990) 156.
[26] D. Buttard, G. Dolino, C. Faivre, A. Halimaoui, F. Comin, V. Formoso, L. Ortega, J. Appl. Phys. 85 (1999) 7105.
[27] T.L.S.L. Wijesinghe, E.J. Teo, D.J. Blackwood, Electrochim. Acta 53 (2008) 4381.
[28] D.K. Bowen, B.K. Tanner, High Resolution X-ray Diffractometry and Topography, Taylor & Francis, London, 1998.
[29] V. Lehmann, Electrochemistry of Silicon: Instrumentation, Science, Materials and Applications, Wiley-VCH Verlag, Weinheim, 2002.
[30] X.G. Zhang, J. Electrochem. Soc. 151 (2004) C69.
[31] H.J. Lewerenz, M. Aggour, C. Murrell, M. Kanis, H. Jungblut, J. Jakubowicz, P.A. Cox, S.A. Campbell, P. Hoffmann, D.S. Schmeisser, J. Electrochem Soc. 150 (2003) E185.
[32] T.L.S.L. Wijesinghe, S.Q. Li, D.J. Blackwood, J. Phys. Chem. C 112 (2008) 303.
[33] L.T. Canham, A.G. Cullis, C. Pickering, O.D. Dosser, T.I. Cox, T.P. Lynch, Nature 368 (1994) 133.
[34] G. Kissinger, J. Vanhellemont, E. Simon, C. Claeys, H. Richter, Mater. Sci. Eng. B 36 (1996) 225.
[35] H. Sugiyama, O. Nittono, Jpn. J. Appl. Phys. 28 (1989) L2013.
[36] A.R. Chelyadinsky, A.M. Dorofeev, N.M. Kazuchits, S. La Monica, S.K. Lazarouk, G. Maiello, G. Masini, N.M. Penina, V.F. Stelmakh, J. Electrochem. Soc. 144 (1997) 1463.
[37] G. Dolino, D. Bellet, Thin Solid Films 255 (1995) 132.
[38] G. Dolino, D. Bellet, C. Faivre, Phys. Rev. B 54 (1996) 17919.
[39] M.V. Wolkin, J. Jorne, P.M. Fauchet, Phys. Rev. Lett. 82 (1999) 197.
[40] J. Kucytowski, K. Wokulska, Cryst. Res. Tech. 40 (2005) 424.